Int. J. Therm. Sci. (1999) 38, 75–88

Application of a general non-dimensional mathematical model to cooling towers

Boris Halasz

Department of Thermodynamics, Faculty of Mechanical Engineering and Naval Architecture, University of Zagreb, Ulica I. Lucica 5, HR-10000 Zagreb, Croatia

(Received 29 July 1997, accepted 30 June 1998)

Abstract—A general non-dimensional mathematical model of evaporative cooling devices is applied to cooling towers. One of the benefits of the non-dimensional approach is that the water-cooling efficiency of a cooling tower can be expressed as a function of only two variables and plotted in a single diagram for each type of cooling tower. For counterflow and parallel flow towers there is an analytic solution of the set of differential equations; crossflow towers require a numerical solution. The resulting rating procedure of the overall performance of a cooling tower is simple and consists of the adjustment of the assumed straight air saturation line to the real air saturation data. All three types of cooling towers can be rated using the same procedure, if a diagram showing the water-cooling efficiency of the respective type is used. The accuracy of this method is checked by the use of published data and is found to be good for the usual operating conditions, failing only when the water-cooling range is very large. © Elsevier, Paris

fheat transfer / mass transfer / adiabatic evaporation / non-dimensional mathematical model / water-cooling tower

Résumé — Application d'un modèle mathématique général adimensionnel aux tours de refroidissement. Un modèle mathématique général adimensionnel de systèmes de refroidissement évaporatifs est appliqué aux tours de refroidissement. Grâce à cette approche adimensionnelle, l'efficacité de refroidissement de l'eau d'une tour peut être exprimée comme une fonction de deux variables seulement et représentée dans un diagramme unique pour chaque type de tour de refroidissement. Pour des tours à contre-courants ou à co-courants, les équations différentielles sont résolues analytiquement. Pour les tours à courants croisés, on adopte une résolution numérique. La procédure d'évaluation des performances globales des tours est simple. Elle consiste à supposer une variation linéaire de la ligne de saturation de l'air, déterminée à partir des données réelles de l'air saturé. Les efficacités des trois types de tours peuvent être évaluées de la même manière. La validité de la méthode est analysée à partir d'une comparaison avec des données publiées. Un bon accord est trouvé dans les conditions habituelles d'utilisation. En revanche, des différences notables apparaissent lorsque la plage des conditions de refroidissement de l'eau est importante. © Elsevier, Paris

transfert de chaleur / transfert de masse / évaporation adiabatique / modèle adimensionnel / tour de refroidissement d'eau

Nomenclature

$A_{s,O}$	overall area of the water-air interface surface	m^2
$C_{0,j}$	constant of integration ($j = 1,2,3$) in equations (5) to (8)	
c_p	specific heat capacity at constant pressure	$J \cdot kg^{-1} \cdot K^{-1}$
c_w	specific heat capacity of liquid water	$J \cdot kg^{-1} \cdot K^{-1}$
h	specific enthalpy	$J \cdot kg^{-1}$
m_j	roots of the characteristic equation, ($j = 1,2,3$)	
p	pressure	Pa
q_m	mass flow rate	$kg \cdot s^{-1}$
r	heat of vaporisation of water	$J \cdot kg^{-1}$
r_0	heat of vaporisation of water at 0°C	$J \cdot kg^{-1}$
v	specific volume of moist air, per kg dry air	$m^3 \cdot kg_{da}^{-1}$
x	air humidity ratio (moisture content)	$kg_w \cdot kg_{da}^{-1}$
z	non-dimensional parameter defined in equation (9)	

Greek symbols

α	convective heat transfer coefficient	$W \cdot m^{-2} \cdot K^{-1}$
ε_T	temperature efficiency	
ϑ	temperature	°C
σ	mass transfer coefficient	$kg_{da} \cdot m^{-2} \cdot s^{-1}$
Φ	heat flow rate	W
ψ_a	non-dimensional air enthalpy (equation (13))	

Subscripts

a	moist air
da	dry air
i	inlet value
m	mean value (crossflow)
o	outlet value
O	overall value (area)
V	vapour
w	water, at water temperature
WB	wet bulb point value

Superscripts

$''$	refers to saturated air

Parameters introduced in [9] *and used here*

(A.1): $b = \dfrac{x''_w - x_{WB}}{\vartheta_w - \vartheta_{WB}}$ the slope of the straight air saturation line (equation (34) and *figure 3* in [9]) ..... $kg_w \cdot kg_{da}^{-1} \cdot K^{-1}$

(A.2): $B = \dfrac{b\, r_{WB}}{c_{p,a}}$ non-dimensional slope of the straight air saturation line

(A.3): $Le = \dfrac{\sigma\, c_{p,a}}{\alpha}$ Lewis number

(A.4): $W = \dfrac{q_{m,w}\, c_w}{q_{m,a}\, c_{p,a}}$ water to air heat capacity rate ratio

(A.5): $X = U X_O$ non-dimensional co-ordinate, proportional to the water–air interface surface (equation (52) in [9])

(A.6): $X_O = \dfrac{\alpha\, A_{s,O}}{q_{m,a}\, c_{p,a}}$ number of transfer units

(A.7): $\varepsilon_w = \dfrac{\vartheta_{w,i} - \vartheta_{w,o}}{\vartheta_{w,i} - \vartheta_{WB}}$ water-cooling efficiency

(A.8): $\Theta = \dfrac{\vartheta - \vartheta_{WB}}{\vartheta_{a,i} - \vartheta_{WB}}$ non-dimensional temperature

(A.9): $\xi = \dfrac{x - x_{WB}}{x_{WB} - x_{a,i}}$ non-dimensional humidity ratio

1. INTRODUCTION

In a cooling tower, water is cooled by evaporation of part of the water into air. This cooling effect is either assisted or abated by simultaneous convective heat transfer between water and air. Since there is no other participant, the process is called adiabatic.

The accurate differential equations describing such a process can be solved only by a lengthy numerical procedure. Without fast computers, the only way to obtain the necessary results was to simplify these equations to such a degree that they could be solved in a reasonably short time. A loss of accuracy was often a consequence.

The first simple enough model was introduced by Merkel in 1925, [1]. By assuming that Lewis' law applies, $(\sigma\, c_{p,a}/\alpha) = 1$, and by neglecting some items in differential equations, he obtained a simple model with the enthalpy difference as a driving force of the process. The possibility of the graphic presentation of these equations in an h,ϑ-diagram made the model rather popular and intelligible. For many years it remained the only usable model, despite its inaccuracy and the inherent ambiguity of the outlet air enthalpy as a result. Many modifications of the basic Merkel model were introduced later, improving either the solution procedure or its accuracy, [2–5]. Merkel's idea was so generally accepted that its applications became the basis of many national standards for cooling tower rating, design and testing.

With fast computers, simplifications are no longer necessary—accurate differential equations can be solved numerically [6], but the problem of presenting the accurate results in a general form is insurmountable, because the number of influencing parameters is very large.

Therefore, the Merkel model retained its merits of transparency and was even transferred to computers [7, 8].

In this paper adiabatic evaporation processes in cooling towers are analysed in a new way. The basis for this approach was presented in [9] in the form of a general non-dimensional model. The primary objective of this model is the simplicity of the relations between operating parameters in order to offer an intelligible insight into their effect on the behaviour of cooling towers. To obtain the simplest possible non-dimensional model, the assumption that the Lewis number is equal to unity, $Le = (\sigma\, c_{p,a}/\alpha) = 1$, although not introduced in the general non-dimensional model, is used throughout this paper.

Various types of cooling towers are in use today—mechanical (forced or induced draft) and buoyancy driven ones, using various types of packing etc.—but from the viewpoint of mathematical models, they can be classified into three groups:

- counterflow cooling towers,
- crossflow cooling towers,
- parallel flow cooling towers.

Water always flows downwards, while the flow direction of air may be different. As far as differential equations are concerned, the flow direction of air is always chosen as the basic one, so the boundary conditions for air are always the same.

2. COUNTERFLOW COOLING TOWERS

In a counterflow cooling tower water flows downwards and air streams upwards. The given boundary conditions are shown in *figure 1.*

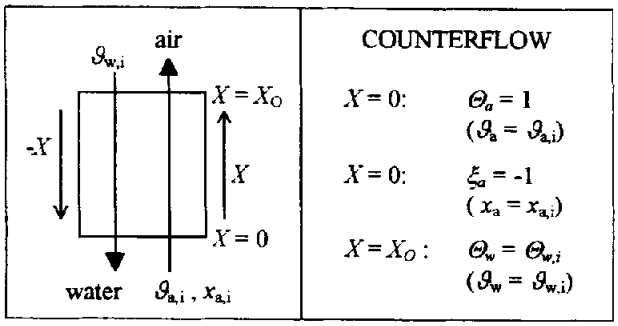

Figure 1. Boundary conditions for counterflow cooling tower.

The equations (54), (55) and (56) in [9], with direction indicator $i_w = -1$ yield a 'normal' set of ordinary differential equations:

$$\frac{d\Theta_a}{dX} = -\Theta_a + \Theta_w \tag{1}$$

$$\frac{d\xi_a}{dX} = -\xi_a + B\,\Theta_w \tag{2}$$

$$\frac{d\Theta_w}{dX} = -\frac{1}{W}\Theta_a - \frac{1}{W}\xi_a + \frac{1+B}{W}\Theta_w \tag{3}$$

There are two *separate* 'driving forces' of the process: temperature difference $(\Theta_w - \Theta_a)$ for the (sensible) heat transfer, and humidity ratio difference $(B\Theta_w - \xi_a) = (\xi''_w - \xi_a)$ for the mass transfer between water and air.

The characteristic equation is of third degree with three roots:

$$m_1 = 0;\ m_2 = \frac{1+B}{W} - 1 \quad \text{and} \quad m_3 = -1 \tag{4}$$

The root m_2 can be a positive or negative number. Since B and W are independent values, $m_2 = 0$ may happen only by coincidence.

The general solution is (for $m_2 \neq 0$):

$$\Theta_a = C_{0,1} + \frac{W}{1+B}\,C_{0,2}\,e^{m_2 X} + C_{0,3}\,e^{-X} \tag{5}$$

$$\xi_a = B\,C_{0,1} + \frac{BW}{1+B}\,C_{0,2}\,e^{m_2 X} - C_{0,3}\,e^{-X} \tag{6}$$

$$\Theta_w = C_{0,1} + C_{0,2}\,e^{m_2 X} \tag{7}$$

Boundary conditions determine constants $C_{0,1}$, $C_{0,2}$ and $C_{0,3}$:

$$\begin{bmatrix} 1 & \frac{W}{1+B} & 1 \\ B & \frac{BW}{1+B} & -1 \\ 1 & e^{m_2 X_O} & 0 \end{bmatrix} \cdot \begin{bmatrix} C_{0,1} \\ C_{0,2} \\ C_{0,3} \end{bmatrix} = \begin{bmatrix} 1 \\ -1 \\ \Theta_{w,i} \end{bmatrix} \tag{8}$$

Equations (5), (6) and (7) yield Θ_a, ξ_a and Θ_w as functions of X, $(0 \le X \le X_O)$, i.e. their distribution within the device. However, if only their *outlet* values are needed, or the water-cooling efficiency ε_w is the only required result, a much simpler procedure can be developed.

For this purpose, a new combined non-dimensional parameter z can be defined:

$$z = \frac{1+B}{W} = \frac{q_{m,a}\,c_{p,a} + q_{m,a}\,r_{WB}\,\dfrac{x''_w - x_{WB}}{\vartheta_w - \vartheta_{WB}}}{q_{m,w}\,c_w} \tag{9}$$

as the ratio of total (i.e. sensible + latent) heat capacity rate of the given mass flow rate of air along its saturation line to the heat capacity rate of the given water mass flow rate. The numerator in equation (9) is fictitious (air does not assume such a state), but is easily imagined in either psychrometric or h,x-diagrams. Through equation (A.2) the parameter B depends upon the inlet air wet bulb temperature ϑ_{WB} and the water temperature in the process. For the given water-to-air mass flow rate ratio W, the magnitude of z increases with the increase of any of these temperatures.

Using the parameter z, a very simple formula for the water-cooling efficiency ε_w is obtained:

$$\varepsilon_w = \frac{\vartheta_{w,i} - \vartheta_{w,o}}{\vartheta_{w,i} - \vartheta_{WB}} = 1 - \frac{\Theta_{w,o}}{\Theta_{w,i}} = z\,\frac{1 - e^{-(1-z)X_O}}{1 - z\,e^{-(1-z)X_O}} \tag{10}$$

which can be plotted in a single diagram (*figure 2*). This figure clearly shows the effect of the two parameters, z and X_O, on the water-cooling efficiency. The 'number of transfer units' X_O, equation (A.6), depends upon the convective heat transfer coefficient α and water-air contact area $A_{s,O}$. Equation (10) also shows that the limit of ε_w for $X_O \to \infty$ is $\varepsilon_{w,max} = z$ when $z \le 1$ and $\varepsilon_{w,max} = 1$ when $z \ge 1$.

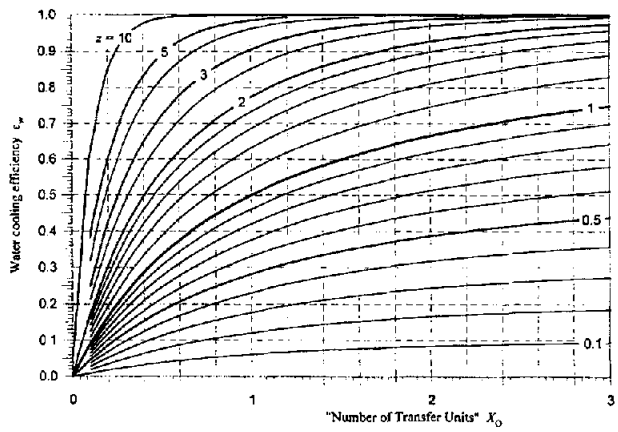

Figure 2. The water cooling efficiency ε_w of a counterflow cooling tower, $Le = 1$.

Equation (10) strongly resembles the expression for the 'temperature efficiency' ε_T of the counterflow *recuperative* heat exchanger [10]. (One must take into account that for recuperators a convention $C_{\min}/C_{\max} \leq 1$ is used and ε_T always refers to the '$C_{\min}$' flow, while the water cooling efficiency ε_w always refers to water, no matter which flow is a '$C_{\min}$' one). Therefore the value of ε_w can be also converted from the 'ε_T *NTU*' diagram of a counterflow *recuperator*:

– if $z < 1$, 'saturated air' is a '$C_{\min}$' flow and water a '$C_{\max}$' flow. Then z corresponds to $C_{\min}/C_{\max}$, X_O can be substituted for *NTU*, but ε_T taken from 'ε_T–*NTU*' diagram must be multiplied by z to yield ε_w: $\varepsilon_w = z\,\varepsilon_T$.

– if $z > 1$, water is a '$C_{\min}$' flow and 'saturated air' is a '$C_{\max}$' flow. Then $1/z$ corresponds to $C_{\min}/C_{\max}$, $(z\,X_O)$ must be substituted for *NTU*, while ε_T taken from 'ε_T–*NTU*' diagram is *equal* to ε_w defined in equation (10)!

In this way a kind of connection between cooling towers and recuperative heat exchangers is established (a similar idea was suggested in [11]).

The model with $Le = 1$ has an interesting feature: if a new variable $\psi_a = \Theta_a + \xi_a$ is introduced[1], the system of three equations, (1), (2) and (3), can be reduced to two equations:

$$\frac{d\psi_a}{dX} = -\psi_a + (1+B)\,\Theta_w \tag{11}$$

$$\frac{d\Theta_w}{dX} = \frac{1}{W}[-\psi_a + (1+B)\,\Theta_w] = \frac{1}{W}\,\frac{d\psi_a}{dX} \tag{12}$$

The new variable ψ_a is, in fact, a non-dimensional enthalpy of air or, more precisely:

$$\psi_a = \Theta_a + \xi_a = \frac{h_a - h_{WB}}{c_{p,a}\,(\vartheta_{a,i} - \vartheta_{WB})} \tag{13}$$

while the second term on the right side of equation (11) can be rewritten as:

$$(1+B)\,\Theta_w = \Theta_w + \xi''_w = \frac{h''_w - h_{WB}}{c_{p,a}\,(\vartheta_{a,i} - \vartheta_{WB})} \tag{14}$$

showing that equations (11) and (12) are the *non-dimensional equivalents* of the famous Merkel equations, but with a linearised air saturation line. These equations also prove that the process in a cooling tower can be, but does not necessarily have to be, expressed as a function of enthalpy as the single driving force of the process! Therefore, the proposed model does not lose information on air temperature and humidity ratio as separate values, as Merkel's model does.

Using equation (13), an overall non-dimensional energy balance, valid for all types of cooling towers for $Le = 1$, can be written:

$$\psi_{a,o} = \psi_{a,o} - \psi_{a,i} = \frac{(1+B)\,\Theta_{w,i}\,\varepsilon_w}{z} = W(\Theta_{w,i} - \Theta_{w,o}) \tag{15}$$

This energy balance is affected by the assumption $q_{m,w}$ = constant and yields a *little smaller* outlet air enthalpy than it should really be.

2.1. Adaptation of the non-dimensional model to the actual process

All the above equations belong to the non-dimensional domain and offer a very clear insight into the effect of the two parameters, z and X_O, governing the whole process. Although the effect of B (within z) is visible in *figure 2*, its numerical value is unknown yet. In fact B, is a link between the real and non-dimensional domain. Through *figure 2*, B depends on the non-dimensional parameters governing the process in a cooling tower. On the other hand, through equations (A.1) and (A.2), B is a function of the inlet air wet bulb temperature ϑ_{WB}, a representative water temperature ϑ_w and air saturation data. For the water-cooling efficiency ε_w of a real cooling tower to be calculated, the magnitude of B valid for the particular process is to be determined. This means that the relations valid in the non-dimensional domain must be adjusted to the real air saturation data to yield the final (dimensional) results.

The following procedure of determining the representative water temperature ϑ_w and the values of b and B was adopted.

It can be shown that equations (11) and (12), with a straight air saturation line implicitly assumed, can be transformed back to dimensional form and integrated over the whole water–air interface surface $A_{s,O}$ to yield an expression:

$$\frac{\sigma\,A_{s,O}}{q_{m,w}\,c_w} = \int_0^{A_{s,O}} \frac{\sigma\,dA_s}{q_{m,w}\,c_w} = \int_{\vartheta_{w,o}}^{\vartheta_{w,i}} \frac{d\vartheta_w}{h''_w - h_a} \tag{16}$$

The *same* equation (but with a real air saturation line!) is already known from Merkel's model. The basic idea is: an 'equivalent' straight air saturation line should produce the same integral on the right-hand side of equation (16) as is obtained with a real saturation line.

The different relationships between water temperature and saturated air enthalpy h''_w, expressed by the straight and the real air saturation lines, will obviously have an effect on the process in a cooling tower, and will cause a slightly different distribution of air enthalpy h_a along the surface as a consequence. However, it will be assumed here that in both cases, h_a is the same function of ϑ_w. These two integrals can be then substantially simplified:

$$\int_{\vartheta_{w,o}}^{\vartheta_{w,i}} (h''_w)_L\,d\vartheta_w = \int_{\vartheta_{w,o}}^{\vartheta_{w,i}} (h''_w)_R\,d\vartheta_w \tag{17}$$

[1] Note that its inlet value is zero, $\psi_{a,i} = \Theta_{a,i} + \xi_{a,i} = 1 - 1 \equiv 0$!

TABLE I
Numerical values of $\Im(\vartheta_w)$ for a total pressure $p = 1$ bar.

ϑ_w °C	$\Im(\vartheta_w)$ kJ·°C·kg^{-1}	ϑ_w °C	$\Im(\vartheta_w)$ kJ·°C·kg^{-1}	ϑ_w °C	$\Im(\vartheta_w)$ kJ·°C·kg^{-1}	ϑ_w °C	$\Im(\vartheta_w)$ kJ·°C·kg^{-1}
1	10.425	16	412.635	31	1 498.820	46	3 886.370
2	22.605	17	459.335	32	1 607.670	47	4 118.170
3	36.595	18	509.070	33	1 722.320	48	4 362.820
4	52.450	19	561.980	34	1 843.020	49	4 620.070
5	70.230	20	618.190	35	1 970.070	50	4 890.620
6	89.995	21	677.825	36	2 103.770	51	5175.270
7	111.800	22	741.040	37	2 244.420	52	5 474.770
8	135.715	23	807.980	38	2 392.370	53	5 789.870
9	161.815	24	878.800	39	2 548.020	54	6 121.470
10	190.180	25	953.675	40	2 711.720	55	6 470.570
11	220.885	26	1 032.790	41	2 883.870	56	6 838.170
12	254.010	27	1 116.330	42	3 064.920	57	7 225.270
13	289.650	28	1 204.495	43	3 255.270	58	7 632.970
14	327.900	29	1 297.490	44	3 455.420	59	8 062.570
15	368.860	30	1 395.520	45	3 665.920	60	8 515.420

where the subscripts 'L' and 'R' denote 'linear' and 'real' respectively.

The real enthalpy of the saturated air $(h''_w)_R$ is a known function of ϑ_w (for the given total pressure p) and can be easily integrated. The integral on the right side of equation (17) can be rewritten as:

$$\Im = \int_{\vartheta_{w,o}}^{\vartheta_{w,i}} h''_w \, d\vartheta_w = \Im(\vartheta_{w,i}) - \Im(\vartheta_{w,o}) \qquad (18)$$

where $\Im(\vartheta_{w,i})$ and $\Im(\vartheta_{w,o})$ can be read from *table I* or calculated using polynomial coefficients quoted in *table II*, for $p = 1$ bar:

$$\Im(\vartheta_w) = a_0 + a_1\,\vartheta_w + a_2\,\vartheta_w^2 + a_3\,\vartheta_w^3 \quad (\text{kJ}\cdot^\circ\text{C}\cdot\text{kg}^{-1}) \quad (19)$$

For pressures considerably different from 1 bar, equation (18) must be integrated, using appropriate values of $h''_w(\vartheta_w, p)$. In this way, the effect of the elevation above sea level can be taken into account by using the appropriate pressure.

On the left-hand side of equation (17), $(h''_w)_L$ is an air enthalpy along the *straight* air saturation line, as defined by equations (33) and (40) in [9]:

$$(h''_w)_L = c_{p,da}\,\vartheta_w + [x_{WB} + b(\vartheta_w - \vartheta_{WB})](r_0 + c_{p,V}\,\vartheta_w) \qquad (20)$$

Here x_{WB} is the real inlet air wet bulb humidity ratio for the given pressure p (or elevation).

TABLE II
Polynomial coefficients for equation (19) for a total pressure $p = 1$ bar.

ϑ_w (°C)	a_0	a_1	a_2	a_3
$5 < \vartheta_w \le 20$	−0.672969	10.0723	0.756563	0.0143143
$20 < \vartheta_w \le 40$	−294.945	48.4703	−0.952424	0.040481
$40 < \vartheta_w \le 60$	−7020.16	520.79	−12.0867	0.128689

If (20) is substituted into left side of equation (17), with $\vartheta_{w,m} = (\vartheta_{w,i} + \vartheta_{w,o})/2$ and with $c_{p,a} \cong c_{p,da} + x_{WB}\,c_{p,V}$ as a specific heat capacity of saturated air, the parameter b is obtained:

$$b = \frac{\dfrac{\Im(\vartheta_{w,i}) - \Im(\vartheta_{w,o})}{\vartheta_{w,i} - \vartheta_{w,o}} - (x_{WB}\,r_0 + c_{p,a}\,\vartheta_{w,m})}{c_{p,V}\left(\dfrac{4\,\vartheta_{w,m}^2 - \vartheta_{w,i}\,\vartheta_{w,o}}{3} - \vartheta_{WB}\,\vartheta_{w,m}\right) + r_0(\vartheta_{w,m} - \vartheta_{WB})} \qquad (21)$$

The rough estimation of b can be made quickly in *figure 3* by drawing a straight line from the point **WB'** (as determined by ϑ_{WB}) on the curved upper line so that between temperatures $\vartheta_{w,o}$ and $\vartheta_{w,i}$, and between a curved line and a straight line, two 'triangular' surfaces of the same area appear. The points **W'** and **WB'** obtained in this manner are transferred vertically down to the lower line to determine points **W** and **WB**. Then a straight line, with slope determined by these

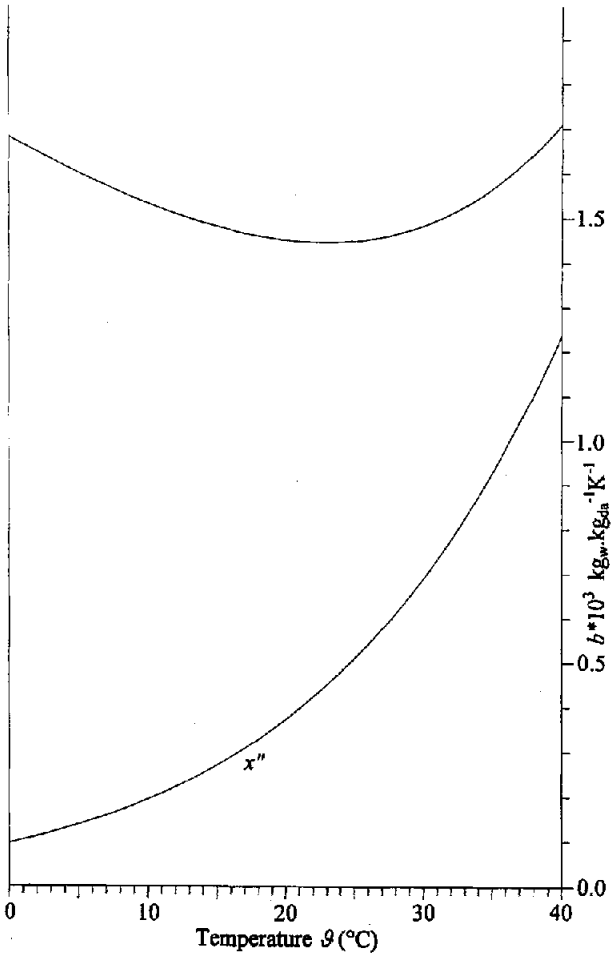

Figure 3. Diagram to determine a value of b. Total pressure $p = 1$ bar.

two points, from the origin of the diagram to the boundary scale, determines b. This graphic procedure is approximate, because $(h''_w)_L$ in equation (20) is not exactly a linear function of ϑ_w. An illustration of the procedure is shown in *figure 4*.

Obviously, the intersection of curved and straight air saturation line (point **W** and the related representative water temperature ϑ_w) lies between $\vartheta_{w,o}$ and $\vartheta_{w,i}$. This diagram also reveals the limitations of the linearised model.

1) The linearisation of the air saturation curve in [9] was introduced assuming that the water temperature change is small. If the cooling range $(\vartheta_{w,i} - \vartheta_{w,o})$ is *very large*, deviation of the straight saturation line from the real one is significant and the assumption introduced for equation (17), concerning the air enthalpy h_a, can be invalid. The non-dimensional model can yield results for such conditions, but their accuracy is likely to be unsatisfactory.

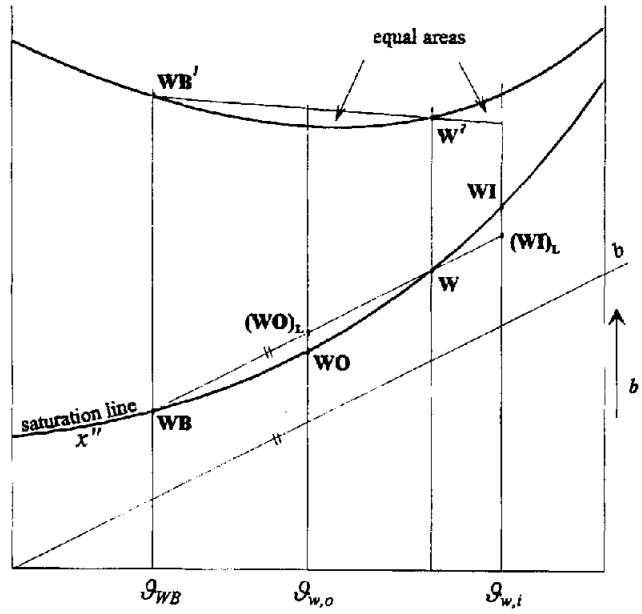

Figure 4. An illustration of the graphic procedure for *figure 3* (not to scale!).

2) As evident from *figure 4*, the distance between points $(\mathbf{WI})_L$ and **WB** is always a little *smaller* than the distance between points **WI** and **WB**, so that the *maximum possible* air enthalpy rise $(h_{a,o} - h_{a,i})_{max} = (h_{a,WI} - h_{a,i})$ is a *little smaller* for the linearised model than it is for the real process. Therefore, a linear non-dimensional model cannot describe a cooling tower operating in such extreme conditions (with *very minimum* air flow), a process when outlet air is saturated at water inlet temperature $\vartheta_{w,i}$. Applying the linearised model to such a situation would lead to $\varepsilon_w > z$, something that is impossible within the non-dimensional model, equation (10).

However, neither of these two operating conditions in cooling towers is typical and the merits of the non-dimensional model should not be judged by these extreme conditions.

There is one more limitation of the non-dimensional model: air is assumed to be unsaturated or, as a limiting case, saturated without fog, equation (40) in [9]. Because of the straight air saturation line, air can never enter the foggy region during the process.

2.2. Outlet air condition, percentage of evaporated water

Once the values of the parameters z, X_O and ε_w are adjusted to the real air saturation data as described in section 2.1 (either by iteration if any of the temperatures $\vartheta_{w,i}$, $\vartheta_{w,o}$ or ϑ_{WB} are to be found for the given X_O, or by a straightforward procedure if X_O must be calculated

for the given temperatures $\vartheta_{w,i}$, $\vartheta_{w,o}$ and ϑ_{WB}), non-dimensional outlet air temperature and humidity ratio can be calculated simply by substituting the values of B and X_O into equations (5) (7), or directly from equations:

$$\Theta_{a,o} = \frac{\Theta_{w,i}\,\varepsilon_w}{z} + e^{-X_O} = \frac{W}{1+B}(\Theta_{w,i} - \Theta_{w,o}) + e^{-X_O} \quad (22)$$

$$\xi_{a,o} = \frac{B\,\Theta_{w,i}\,\varepsilon_w}{z} - e^{-X_O} = \frac{BW}{1+B}(\Theta_{w,i} - \Theta_{w,o}) - e^{-X_O} \quad (23)$$

Actual (dimensional) outlet air temperature and humidity ratio can be obtained either by conversion of these values by the use of equations (A.8) and (A.9), or directly from:

$$\vartheta_{a,o} = \vartheta_{WB} + \left[\frac{1}{z}(\vartheta_{w,i} - \vartheta_{w,o}) + (\vartheta_{a,i} - \vartheta_{WB})e^{-X_O}\right] \quad (24)$$

$$x_{a,o} = x_{WB} + (x_{WB} - x_{a,i})\left[\frac{B}{z}\frac{\vartheta_{w,i} - \vartheta_{w,o}}{\vartheta_{a,i} - \vartheta_{WB}} - e^{-X_O}\right] \quad (25)$$

One peculiar problem is encountered when inlet air is saturated: equation (10) can still be used, but since $(\vartheta_{a,i} - \vartheta_{WB}) = 0$ and $(x_{WB} - x_{a,i}) = 0$, the non-dimensional values $\Theta_{a,o}$ and $\xi_{a,o}$ are undetermined. However, their actual values $\vartheta_{a,o}$ and $x_{a,o}$ can be calculated as:

$$\vartheta_{a,o} = \vartheta_{WB} + \frac{\varepsilon_w}{z}(\vartheta_{w,i} - \vartheta_{WB}) \quad (26)$$

$$x_{a,o} = x_{WB} + b(\vartheta_{a,o} - \vartheta_{WB}) \quad (27)$$

Finally, if needed, the percentage of evaporated water and the ratio of total rejected heat flow rate to the one rejected by evaporation alone, as defined by equations (67) and (69) in [9], can be calculated:

$$\frac{\Delta q_{m,w}}{q_{m,w}} = \frac{c_w(\vartheta_{a,i} - \vartheta_{WB})}{r_{WB}}\,\frac{1+\xi_{a,o}}{W} \quad (28)$$

$$\kappa = 1 + \frac{\Theta_{a,o} - 1}{1+\xi_{a,o}} = \frac{W(\Theta_{w,i} - \Theta_{w,o})}{1+\xi_{a,o}} \quad (29)$$

The overall rating procedure described in sections 2.1 and 2.2 is rather simple and its great advantage is that the same above relations are valid for all three types of cooling towers (for crossflow cooling towers they yield *mean outlet values* $\vartheta_{w,o,m}$, $\vartheta_{a,o,m}$ and $x_{a,o,m}$). The only difference will be contained within the respective diagrams $\varepsilon_w = \varepsilon_w(X_O, z)$! This is of great benefit for crossflow cooling towers.

2.3. Illustration of the results

Two examples illustrate the complete results produced by the non-dimensional model and transformed to real values. Common input:

$\vartheta_{w,i} = 32\ ^\circ C$; $\vartheta_{WB} = 20\ ^\circ C$; $\vartheta_{a,i} = 35\ ^\circ C$;
($p = 1$ bar; $x_{a,i} = 0.00856\ kg \cdot kg^{-1}$), $X_O = 3$

The results, quoted in *table III* and plotted in *figures 5* and *6*, offer quite detailed information about the process. It should be remembered that the co-ordinate X in *figure 5* is not necessarily exactly proportional to the physical height of the cross-section in a tower.

TABLE III
Computed values for *figures 5* and *6*.

Calculated item:	example 'a'	example 'b'
Required $\vartheta_{w,o}$ (°C)	27	22
ε_w, equation (10)	0.417	0.833
z, equation (10)	0.474	1.205
B, equation (A.2)	2.988	2.862
W, equation (A.4)	8.421	3.204
x, equation (29)	1.160	0.843
$\Delta q_{m,w}/q_{m,w}$ (%) equation (28)	0.735	2.024

The opposite curvature of the ϑ_w-lines in *figure 5* is a consequence of the characteristic equation root m_2 of opposite sign in these two examples.

The dimensional values, calculated at regular intervals of X, were transferred to the psychrometric chart (*figure 6*). The pairs of data (ϑ_w, x''_w) follow the straight air saturation line.

2.4. Testing the results using the published data

Undoubtedly the best test of the accuracy of the non-dimensional model would be to conduct a series of measurements on a test facility designed for the purpose. Since at the present this option is not available to the author, some published results were used to perform the preliminary check of the accuracy of the new non-dimensional model.

In doing this, two sources of reference data were used: accurate numerical solutions of the accurate differential equations, and manufacturer's bulletins based on presumably very extensive experimental data.

In [6], a detailed analysis of heat and mass transfer processes in cooling towers is given together with a number of results, obtained by the numerical solution of rather accurate differential equations.

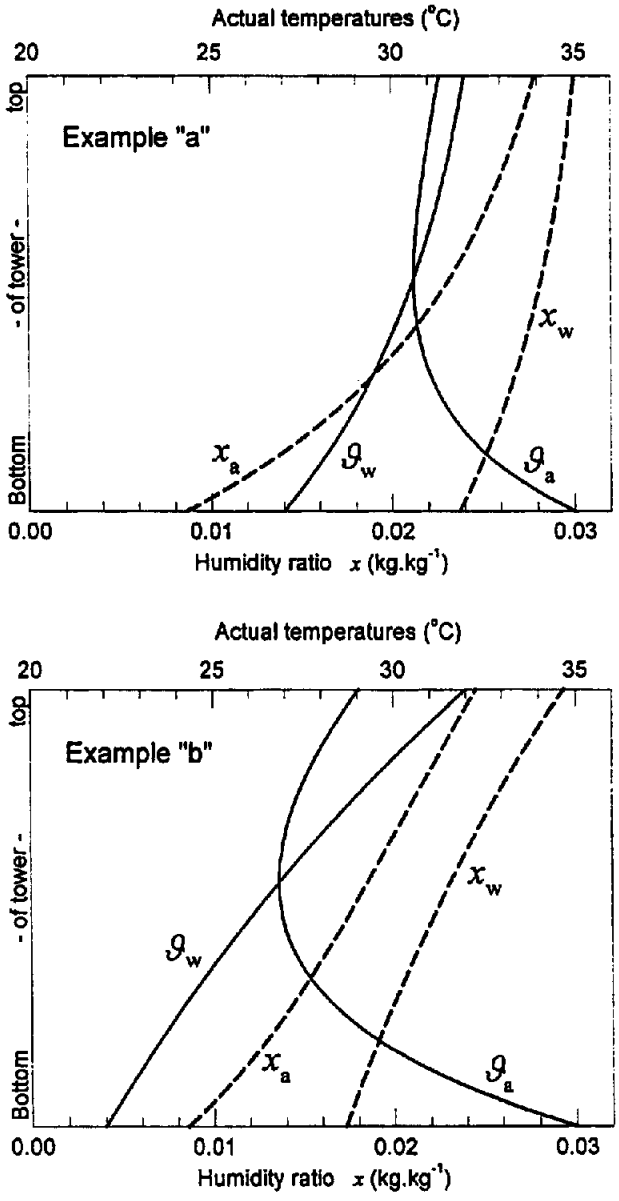

Figure 5. Temperature and humidity ratio distribution within the cooling tower. Above: example 'a', below: example 'b'.

In *table IV*, a list of results is given. First, the complete *table II* from [6] is repeated (columns 1 to 10). Then, in columns 11 to 14, results obtained by the non-dimensional model (with $Le = 1$) are quoted.

The N_G value, used in [6], can be easily converted to X_O:

$$N_G = \frac{\sigma A_{s,O}}{q_{m,a}} = \frac{\sigma c_{p,a}}{\alpha} \frac{\alpha A_{s,O}}{q_{m,a} c_{p,a}} = Le\, X_O = X_O \quad (30)$$

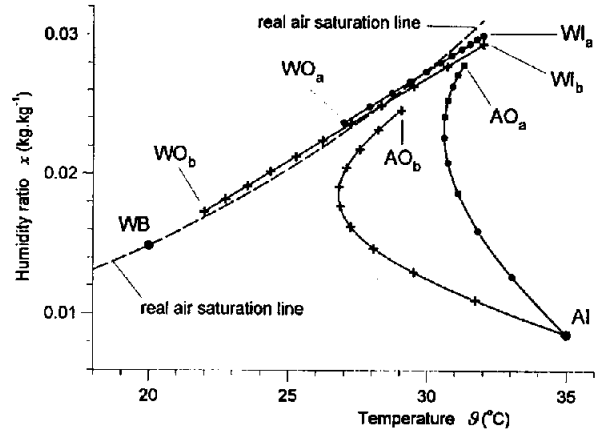

Figure 6. Air condition change. Examples 'a' and 'b'.

The results of the non-dimensional model (column 11) appear rather accurate (better than those of the Merkel model) for the input data No. 0.1 to 5.3, with an error of only a few percent!

The rest of results (No. 6.1 to 8.4) are inaccurate, but the 'cooling ranges' ($\vartheta_{w,i} - \vartheta_{w,o}$) are so large (20 or 30 °C!) and the 'approaches' ($\vartheta_{w,o} - \vartheta_{WB}$) are so small in these examples, that the linearisation obviously introduces too large an error!

For input data No. 1.1 and 4.1 the new model yields no results, since here $\varepsilon_w > z$. Outlet air temperature (33.62 °C and 33.51 °C) is too near to the water inlet temperature (34 °C), as mentioned in connection with *figure 4*.

However, the examples No. 6.1 to 8.4 and No. 1.1 or 4.1 just coincide with the above-mentioned limitations of the new model! So, apart from these extreme situations, linearised non-dimensional model seems to produce very acceptable results for X_O.

As far as the air outlet condition ($\vartheta_{a,o}$ and $x_{a,o}$) is concerned, the results of the non-dimensional model can be considered as satisfactory in general. Larger deviations of the results in columns 13 and 14 from accurate results (columns 6 and 7) can be found in the examples marked with an asterisk, but in these very examples the outlet air condition, computed with an accurate model, is foggy! Since in deriving the non-dimensional model a formula for the enthalpy of unsaturated air was used, equation (40) in [9], an error is inevitable. Nevertheless, the outlet air enthalpy is computed fairly accurately even with the non-dimensional model (energy balance!). Also the outlet humidity ratio is acceptable (although always slightly smaller) in these examples, but its temperature is significantly lower than it should be. In general, the outlet condition obtained in equations (24) and (25) should be checked: if the outlet air temperature and humidity ratio indicate foggy conditions, the outlet air enthalpy and humidity ratio can be accepted, while the outlet air temperature should be corrected.

TABLE IV
Comparison of the results for the counterflow cooling tower.

	Input data					Accurate model			Merkel		Non-dimensional model			
No.	1 $\vartheta_{w,i}$ °C	2 $\vartheta_{w,o}$ °C	3 $\vartheta_{a,i}$ °C	4 ϑ_{WB} °C	5 $\frac{q_{m,a}}{q_{m,w}}$	6 $\vartheta_{a,o}$ °C	7 $x_{a,o}$ g·kg^{-1}	8 N_G	9 N_{GM}	10 $\Delta\%$	11 X_O (= N_G)	12 $\Delta\%$	13 $\vartheta_{a,o}$ °C	14 $x_{a,o}$ g·kg^{-1}
0.1	30	26	8	4	0.25	27.01*	23.39*	2.119	1.900	−10.4	2.106	−0.6	26.57	22.73
0.2	30	26	8	4	0.30	24.36*	20.09*	1.396	1.283	−8.1	1.358	−2.7	23.43	19.49
0.3	30	26	8	8	0.30	26.28*	22.61*	1.777	1.615	−9.1	1.746	−1.8	25.30	22.09
1.1	34	30	16	12	0.20	33.62*	34.22*	4.707	3.422	−27.3	–	–	-	–
1.2	34	30	16	12	0.25	30.63*	28.89*	1.861	1.666	−10.5	1.848	−0.7	30.32	28.29
1.3	34	30	16	12	0.30	28.36*	25.29*	1.275	1.167	−8.5	1.247	−2.2	27.90	24.73
1.4	34	30	16	16	0.30	30.49*	28.85*	1.706	1.540	−9.7	1.684	−1.3	29.76	28.37
2.1	34	30	24	20	0.30	32.72	32.45	2.913	2.484	−14.7	3.070	+5.4	32.97	32.10
2.2	34	30	24	20	0.35	31.30	29.75	1.872	1.680	−10.3	1.875	+0.2	31.57	29.40
2.3	34	30	24	20	0.40	30.34	27.71	1.419	1.295	−8.7	1.405	−1.0	30.57	27.40
2.4	34	30	24	24	0.40	32.82	32.66	2.955	2.561	−13.3	3.040	+2.9	32.87	32.42
3.1	34	30	32	28	0.80	32.48	31.05	2.073	1.880	−9.3	2.075	+0.1	32.58	31.02
3.2	34	30	32	28	1.00	32.20	29.45	1.393	1.287	−7.6	1.386	−0.5	32.26	29.42
3.3	34	30	32	28	1.20	32.08	28.36	1.056	0.984	−6.9	1.049	−0.7	32.12	28.35
4.1	34	24	16	12	0.50	33.51	33.97	7.154	5.446	−23.9	–	–	–	–
4.2	34	24	16	12	0.80	27.52*	23.98*	1.564	1.456	−6.9	1.544	−1.3	27.50	23.54
4.3	34	24	16	12	1.00	25.11	20.63	1.086	1.020	−6.1	1.054	−3.0	25.11	20.27
4.4	34	24	16	16	1.00	27.54*	24.23*	1.497	1.397	−6.7	1.444	−3.5	26.90	23.92
5.1	34	24	24	20	1.00	30.07	27.74	2.603	2.404	−7.6	2.534	−2.7	30.38	27.52
5.2	34	24	24	20	1.50	27.66	23.02	1.284	1.211	−5.7	1.223	−4.7	27.88	22.88
5.3	34	24	24	20	2.00	26.65	20.60	0.861	0.817	−5.1	0.817	−5.1	26.80	20.51
6.1	40	20	16	12	1.50	28.21*	25.19*	1.560	1.489	−4.6	1.399	−10.3	27.62	24.90
6.2	40	20	16	12	2.00	25.06*	20.70*	1.031	0.988	−4.2	0.918	−11.0	24.57	20.53
6.3	40	20	16	12	3.00	21.61	16.20	0.617	0.593	−3.9	0.548	−11.2	21.63	16.09
6.4	40	20	16	16	3.00	24.24*	20.02*	0.875	0.839	−4.2	0.745	−14.9	22.75	19.99
7.1	40	20	22	18	3.00	25.85	21.12	1.162	1.127	−3.0	0.978	−15.8	25.96	21.08
7.2	40	20	22	18	5.00	24.18	17.29	0.623	0.606	−2.7	0.530	−15.0	24.23	17.26
7.3	40	20	22	18	8.00	23.32	15.10	0.368	0.358	−2.6	0.314	−14.6	23.34	15.10
8.1	54	24	16	12	1.00	39.55*	49.36*	2.127	2.037	−4.2	1.732	−18.6	37.63	48.90
8.2	54	24	16	12	1.50	33.50*	35.17*	1.150	1.108	−3.7	0.930	−19.1	30.20	35.00
8.3	54	24	16	12	2.00	29.71*	28.13*	0.792	0.764	−3.6	0.640	−19.2	26.57	28.08
8.4	54	24	16	16	2.00	31.70*	31.95*	0.961	0.926	−3.6	0.749	−22.1	27.55	32.11

Another test of accuracy was performed using the manufacturer's technical bulletin, [12], with an arbitrarily chosen VXT-470 type of cooling tower. Although handicapped by possible errors in reading data from diagrams, the test produces interesting results. For a series of data read from diagrams: inlet air wet bulb temperature (ϑ_{WB}), water ($q_{m,w}$) and air ($q_{m,a}$) mass flow rates, 'cooling range' ($\vartheta_{w,i} - \vartheta_{w,o}$) and 'approach' ($\vartheta_{w,o} - \vartheta_{WB}$), the calculated values of the 'number of transfer units' X_O were plotted in a diagram, showing X_O vs. the ratio ($q_{m,a}/q_{m,w}$) (*figure 7*). This figure shows that, for water cooling ranges up to 15 °C, the values of X_O obtained by the non-dimensional model follow a rather narrow zone, while for 20 °C cooling range the points are significantly lower. This was already noticed in *table IV* (examples 6.1–8.4) and also in [13].

A large scattering of the points is also visible on the leftmost part of the diagram (extremely large water loading), where the relationship between X_O and the ratio ($q_{m,a}/q_{m,w}$) obviously does not exist.

Figure 7 also shows that, although plotted in a log-log scale diagram, the points do not follow the straight 'best fit line', as might be expected from equation (31).

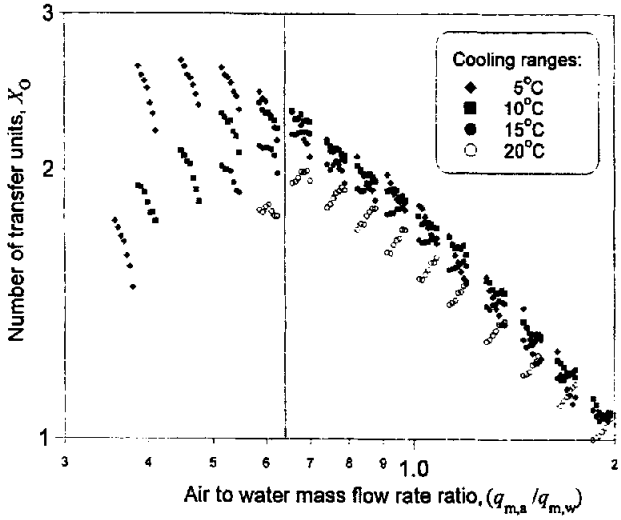

Figure 7. Number of transfer units X_O vs. air to water mass flow rate ratio.

2.5. Simulating the cooling tower operation in various conditions

The difficulties in predicting the performance of the given cooling tower operating under different or variable conditions were solved earlier by drawing the lines of 'available' and 'required' number of transfer units in a diagram [4, 15, 16, 17], intersection of these two lines being a new operating point. The procedure was based on Merkel's model. Recently, this procedure was transferred to computer [8].

The problem is aggravated by the fact that the number of transfer units X_O is changed, even for the same hardware of the device, when any of the operating parameters, particularly water and air mass flow rates, is changed.

As suggested in [18] and commonly quoted, the number of transfer units X_O of a particular cooling tower with given geometry and size of the packing is assumed to depend upon the air to water mass flow rate ratio:

$$X_O = C \left(\frac{q_{m,a}}{q_{m,w}} \right)^n \tag{31}$$

where C and n are constants determined by at least two known operating points. However, the accuracy of equation (31) is known to be questionable [4, 11, 14] (compare with *figure 7*) and its use is recommended for the values of ($q_{m,a}/q_{m,w}$) not far from the measured operating point.

Some other correlations were also proposed in [19, 20], such as:

$$X_O = C\, q_{m,a}^{n_1}\, q_{m,w}^{n_2} \tag{32}$$

which may hopefully cover a greater range of water and air mass flow rates.

Whichever of these correlations is used, with the non-dimensional model, 'simulation' of the cooling tower operation is just one calculation for each given operating condition.

Examples of the rating procedure are given in the Appendix.

3. CROSSFLOW COOLING TOWERS

In the crossflow cooling tower air streams horizontally, while water drops downwards through the packing, not vertically but slightly drifted by the air stream.

The heat and mass transfer process is a two-dimensional problem. Although both water and air enter at uniform temperatures $\vartheta_{w,i}$ and $\vartheta_{a,i}$, various water and air particles undergo different processes and assume different states. The variously cooled particles of water are mixed in a sump to produce a mean outlet water temperature $\vartheta_{w,o,m}$.

The two independent co-ordinates describe the flow directions of air and water:

$$U_a \equiv U \quad \text{and} \quad U_w = V \tag{33}$$

The set of three partial differential equations is obtained by the substitution of U and V into equations (48), (49) and (51) in [9]:

$$\frac{\partial \Theta_a}{\partial U} = -X_O\,\Theta_a + X_O\,\Theta_w \qquad (34)$$

$$\frac{\partial \xi_a}{\partial U} = -X_O\,\xi_a + BX_O\,\Theta_w \qquad (35)$$

$$\frac{\partial \Theta_w}{\partial V} = \frac{X_O}{W}\,\Theta_a + \frac{X_O}{W}\,\xi_a - \frac{X_O}{W}\,(1+B)\,\Theta_w \qquad (36)$$

and can be solved by any appropriate numerical method, using boundary conditions (*figure 8*).

The water-cooling efficiency ε_w depends upon only two parameters, z and X_O (*figure 9*). Compared to *figure 2*, the crossflow cooling tower has a slightly lower performance than the counterflow type.

If the mean outlet values $\vartheta_{a,o,m}$ and $x_{a,o,m}$ are required, the same procedure that was explained for a counterflow cooling tower, equations (22) to (25), can be used.

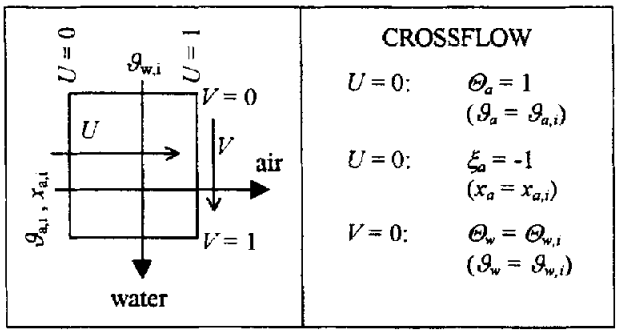

Figure 8. Boundary conditions for crossflow cooling tower.

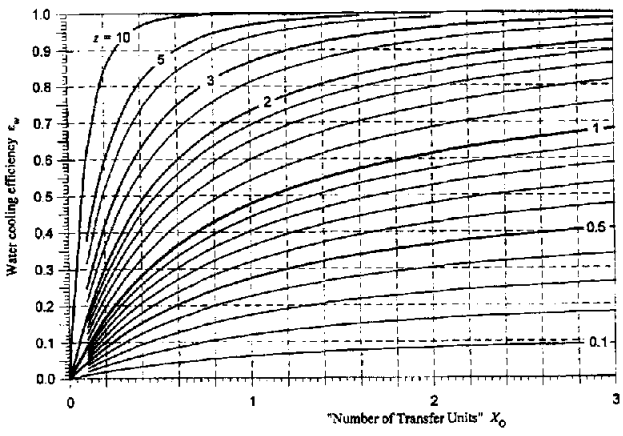

Figure 9. The water cooling efficiency ε_w of a crossflow cooling tower, $Le = 1$.

There is also the same relationship between the crossflow cooling tower and the crossflow recuperative heat exchanger as explained with *figure 2*. Also the overall rating procedure for crossflow cooling towers is the same as the procedure shown in Appendix for the counterflow type, apart from the use of *figure 9*.

3.1. Adaptation of the non-dimensional model to the actual process

The procedure of finding the values b and B, described in section 2.1 for the counterflow cooling towers, can be used here too, and the numerical value of b will be calculated from equation (21), using $\vartheta_{w,o,m}$ for $\vartheta_{w,o}$. The analogy is not complete, because the processes in counterflow and crossflow cooling towers are not the same, but as the difference between their performance is relatively small, results can be expected to be reasonably good.

3.2. Testing the results by the published data

The published results for crossflow cooling tower are sparse. Some results, obtained by solving the set of accurate partial differential equations, can again be found in [6].

In one example, a process was solved using the accurate model and compared to the solution obtained by Merkel's procedure. Results (for the input data $\vartheta_{w,i} = 40$ °C, $\vartheta_{a,i} = 15$ °C, $\vartheta_{WB} = 12$ °C, $q_{m,a}/q_{m,w} = 1$, $N_G = 1$) are quoted in *table V*. In this example, the non-dimensional model yields a very good result for $\vartheta_{w,o,m}$, almost the same as the accurate model, while $\vartheta_{a,o,m}$ and $x_{a,o,m}$ are lower than the results of the accurate model.

The non-dimensional model has a distinctive advantage: to obtain the results in *table V*, either by an accurate or Merkel's model, the *system* of differential equations must be solved. On the contrary, the rating procedure based on the non-dimensional model is much simpler if *figure 9* is used. This advantage would be even more pronounced if the reverse procedure were needed calculation of the required X_O for the given

TABLE V
Comparison of the results for the crossflow cooling tower.

Computed value	1 Accurate (Le = 1,156)	2 Merkel's (Le = 1)	3 Nondim. (Le = 1)
$\vartheta_{w,o,m}$ (°C)	27.6	27.1	27.58
$\vartheta_{a,o,m}$ (°C)	27.3	27.3*	26.78
$x_{a,o,m}$ (g·kg^{-1})	24.4	24.1*	23.70

* Merkel's model yields air enthalpy as the only result!

TABLE VI
Comparison of the results for the crossflow cooling tower.

	Input data						Accurate model			Non-dimensional model			
No.	1 $\vartheta_{w,i}$ °C	2 $\vartheta_{w,o}$ °C	3 $\vartheta_{a,i}$ °C	4 $x_{a,i}$ g·kg^{-1}	5 $q_{m,a}$ kg·h^{-1}	6 $q_{m,w,i}$ kg·h^{-1}	7 $\vartheta_{a,o}$ °C	8 $x_{a,o}$ g·kg^{-1}	9 N_G	10 X_O (= N_G)	11 Δ%	12 $\vartheta_{a,o}$ °C	13 $x_{a,o}$ g·kg^{-1}
10	62	35	15	5.6	273.4	136.1	27.6**	25.4**	0.343	0.28	−18.4	22.81	24.93
11	59	42	15	5.6	410.7	408.2	30.8**	31.2**	0.375	0.335	−10.7	24.84	29.88
12	50	41	15	5.6	319.3	544.3	29.5**	28.4**	0.460	0.42	−8.7	25.48	27.01
13	40	35	15	5.6	321.0	666.8	24.6*	20.3*	0.502	0.47	−6.4	23.46	19.54
14	37.5	31	15	5.6	125.5	122.5	20.4	14.3	0.348	0.33	−5.2	20.43	14.01
15	37	30	15	5.6	146.8	108.9	19.4	12.8	0.297	0.275	−7.4	19.50	12.46
16	39.1	32	18.3	8.9	74.9	108.9	27.0*	23.4*	0.685	0.645	−5.8	26.49	22.31

* slightly foggy condition; ** far beyond saturation line.

$\vartheta_{w,o,m}$. Then the non-dimensional model would give a simple *straightforward solution without iteration*, while both the accurate model and Merkel's procedure would require a *number of repeated complete solutions* of the system of differential equations: X_O should be varied as an input value, until the desired result ($\vartheta_{w,o,m}$) is obtained.

Additional test was performed using data from *table V* in [6] (these data were first quoted in [19] and checked in [6]). The results obtained by the non-dimensional model are listed in *table VI*. The general conclusion is very similar to the one for *table IV*: the non-dimensional model fails when the outlet air condition is foggy, examples No. 10–12, especially for a very large cooling range. The results in examples No. 13–16 are more accurate. The non-dimensional model consistently yields lower temperature and humidity ratio of the outlet air—an error attributable to the linearisation of the air saturation line as well as to the assumption $q_{m,w}$ = const.

However, more data would be needed to estimate the accuracy of the application of the non-dimensional model to crossflow cooling towers.

4. PARALLEL FLOW COOLING TOWERS

The parallel flow cooling tower (*figure 10*) is not a widely-used type of a cooling tower, because equation (37):

$$\varepsilon_w = \frac{z}{1+z}(1 - e^{-(1+z)X_O}) \qquad (37)$$

shows that a parallel flow cooling tower is incapable of matching the performance of any of the other two types for any set of operating conditions.

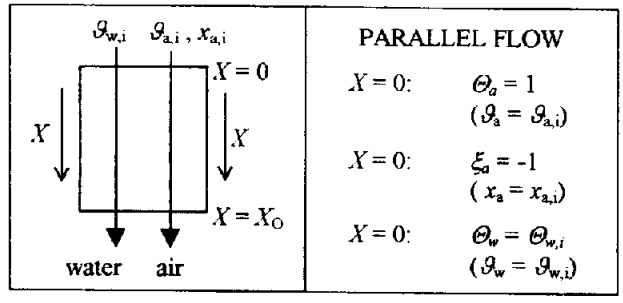

Figure 10. Boundary conditions for parallel flow cooling tower.

Figure 11 very clearly illustrates the 'saturation' effect, a rapid approach of the water-cooling efficiency to the asymptotic value.

5. CONCLUSION

The application of the general non-dimensional model of evaporative cooling devices to cooling towers yields a rather simple rating procedure. This application has some very useful features.

1) It is very simple if $Le = 1$ is assumed. The water-cooling efficiency of a cooling tower can be expressed as a function of only two independent non-dimensional input variables and their effect on the process becomes rather understandable. Furthermore, the water-cooling efficiency ε_w can be computed in advance and can be presented simply in a ε_w, X_O-diagram—a very advantageous feature for rating crossflow cooling towers.

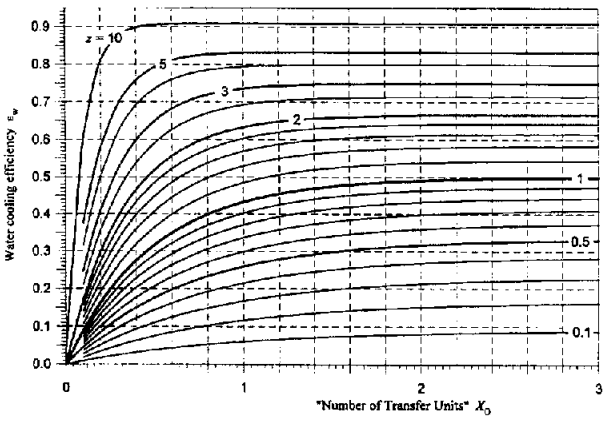

Figure 11. The water cooling efficiency ε_w of a parallel flow cooling tower, $Le = 1$.

2) A unique overall rating procedure for all types of cooling towers based on the respective ε_w, X_O-diagrams can be developed, similar to the unique rating procedure of recuperative heat exchangers. In such a way, a simple and obvious comparison of the water-cooling effectiveness of various types of cooling towers is possible.

3) The accuracy of results is rather good, when moderate operating conditions are considered. Regrettably, the accuracy diminishes, if the linear model is stretched beyond its reasonable limits, i.e. when it is applied to a very large water-cooling range: substitution of a straight line for a very large curved section of a real air saturation line increases the error.

4) Outlet air temperature and humidity ratio can be calculated very simply as separate values (these results are not available at all with Merkel's model)— a feature potentially very useful for natural draught cooling towers, where the density of outlet air must be known.

The application of the general non-dimensional model to cooling towers seems to offer a good compromise of simplicity, accuracy and completeness under moderate operating conditions. However, like all linearised models, the proposed one cannot describe satisfactorily the extreme operating conditions (very large water-cooling ranges, operation with minimum air-flow rate, processes where air assumes foggy condition).

There is probably room for the improvement of the non-dimensional model, concerning its accuracy for the above-mentioned extreme operating conditions, but for this objective a larger number of reliable measured data would be needed.

There is one additional and very interesting feature of this model it links rather than separates various kinds of heat exchangers: through *figures 2, 9* and *11*, water cooling towers are linked with recuperative heat exchangers; through equations (11) and (12), the new model is related to earlier models based on Merkel's idea and, not to be forgotten, as an application of the general non-dimensional model, water cooling towers are just members of the family of evaporative cooling devices.

REFERENCES

[1] Merkel F., Verdunstungskühlung, VDI-Forschungsheft 275 (1925).

[2] Simpson W.M., Sherwood T.K., Performance of Small Mechanical Draft Cooling Tower, Refrigerating Engineering 54 (12) (1946) 535–543.

[3] Mickley H.S., Design of Forced Draft Air Conditioning Equipment, Chemical Engineering Progress 45 (12) (1949) 739–745.

[4] Baker D.R., Shryock H.A., A Comprehensive approach to the analysis of cooling tower performance, J. Heat Trans.–T. ASME 83 (3) (1961) 339–350.

[5] Gardner G.C., Heat- and mass-transfer calculations using an exponentially curved equilibrium line with special reference to cooling towers, Int. J. Heat Mass Tran. 10 (6) (1967) 763–770.

[6] Poppe M., Wärme- und Stoffübertragung bei der Verdunstungskühlung im Gegen- und Kreuzstrom, VDI-Forschungsheft 560 (1973).

[7] Water Cooling Towers, BS 4485, British Standards Institution, 1988.

[8] Webb R.L., Villacres A., Performance Simulation of Evaporative Heat Exchangers (Cooling Towers, Fluid Coolers, and Condensers), Heat Transfer Eng. 6 (2) (1985) 31–38.

[9] Halasz B., General Mathematical Model of Evaporative Cooling Devices, Rev. Gén. Therm. 37 (4) (1998) 245–255.

[10] Bošnjaković F. Nauka o toplini II, Tehnička knjiga, Zagreb, 1976.

[11] Klenke W., Die Kühlturmkennlinie als mittel für die Beurteilung von Kühltürmen, Brennstoff-Wärme-Kraft 18 (3) (1966) 97–105.

[12] VX Cooling Towers, S.I. Metric Bulletin S 280/3-5, Baltimore Aircoil, 1983.

[13] Spangemacher K., Berechnung von Kühltürmen und Einspritzkühlern mit Hilfe einer Verdunstungs-Kennzahl, Brennstoff-Wärme-Kraft 10 (5) (1958) 209–215.

[14] Poppe M., Rögener H., Berechnung von Rückkühlwerken, VDI- Wärmeatlas, 5. Auflage (1988) pp. Mi1-Mi15.

[15] Spangemacher K., Characteristic von Kühltürmen mit natürlichem und künstlichem Zug, Brennstoff-Wärme-Kraft 16 (5) (1964) 241–246.

[16] Rögener H., Auswertung von Abnahmeversuchen an Ventilatorkühltürmen, Brennstoff-Wärme-Kraft 10 (7) (1958) 336–339.

[17] Poppe M., Zur Beurteilung von Gegenstrom-Kühlsystemen, Brennstoff-Wärme-Kraft 25 (2) (1973) 38–42.

[18] Kelly N.W., Swenson L.K., Comparative Performance of Cooling Tower Packing Arrangements, Chem. Eng. Prog. 52 (7) (1956) 263–268.

[19] Molyneux F., Counter- and cross-flow cooling towers, Chem. Proc. Eng. 48 (5) (1967) 56–60.

[20] Thomas W.J., Houston P., Simultaneous heat and mass transfer in cooling towers, British Chemical Engineering 4 (3/4) (1959) 160–163 and 217–222.

APPENDIX

Examples of the rating procedure

The performance of the particular counterflow cooling tower, for the two sets of operating conditions, is given in *table VII*.

TABLE VII
Two operating points of the cooling tower (volume flow rate of air is presumably constant at 51.82 $m^3 \cdot s^{-1}$).

Operating point	1	2
Wet bulb temperature ϑ_{WB} (°C)	26.00*	18.95*
Cooling range (°C)	12.00*	8.00*
Approach (°C)	2.55*	6.50*
Water volume flow rate $q_{v,w}$ ($L \cdot s^{-1}$)	40.06*	78.86*
Water inlet temperature $\vartheta_{w,i}$ (°C)	40.55	33.45
Water outlet temperature $\vartheta_{w,o}$ (°C)	28.55	25.45
Water mass flow rate $q_{m,w}$ ($kg \cdot s^{-1}$)	39.74	78.43
Air mass flow rate $q_{m,a}$ ($kg \cdot s^{-1}$)	58.36	60.47

* Data taken from manufacturer's bulletin. The rest of data calculated using known relations. Mass flow rates calculated using water density at $\vartheta_{w,i}$ and density of saturated air at ϑ_{WB}.

To be calculated:

1) using the data from *table VII*, find the values C and n for equation (31);

2) if operating conditions are changed to: $\vartheta_{a,i}$ = 27 °C, ϑ_{WB} = 21.1 °C, $q_{v,w}$ = 57.41 $L \cdot s^{-1}$ and $\vartheta_{w,i}$ = 42 °C, find the outlet water temperature ($\vartheta_{w,o}$) and outlet air condition ($\vartheta_{a,o}$ and $x_{a,o}$);

3) for the operating conditions given in 2), find $\vartheta_{w,i}$, $\vartheta_{w,o}$, $\vartheta_{a,o}$ and $x_{a,o}$, if the water cooling range must be fixed at $\vartheta_{w,i} - \vartheta_{w,o}$ = 10 °C.

Solution

1) For the two given operating points, X_O can be calculated (*table VIII*):

TABLE VIII
Calculated data for the two operating conditions

r_{WB} $kJ \cdot kg^{-1}$	$c_{p,a}$ $kJ \cdot kg^{-1} \cdot K^{-1}$	B	W	z	ε_w	X_O
2 441.3	1.0468	4.1394	2.716	1.8923	0.8247	1.310
2 457.2	1.0319	2.9442	5.249	0.7514	0.5517	2.103

and, from equation (31): C = 1.7375 and n = −0.7345.

2) For the wet bulb temperature 21.1 °C:

$$x_{WB} = 0.01596 \text{ kg} \cdot \text{kg}^{-1},\ r_{WB} = 2\,452.4 \text{ kJ} \cdot \text{kg}^{-1},$$
$$c_{p,a} = 1.0358 \text{ kJ} \cdot \text{kg}^{-1} \cdot \text{K}^{-1},\ v_{WB} = 0.866 \text{ m}^3 \cdot \text{kg}^{-1},$$

and hence: $q_{m,a}$ = 59.84 $kg \cdot s^{-1}$, $q_{m,w}$ = 56.94 $kg \cdot s^{-1}$,

$$X_O = 1.6752 \text{ and } W = 3.83535$$

Since $\vartheta_{w,o}$ is unknown, iteration is required (*table IX*).

TABLE IX
Iteratively calculated data in example 2.

Item	Step 1	Step 2	Step 3
Assumed value $\vartheta_{w,o}$	30.0	26.843	27.031
b, equation (31)	0.0016166	0.0015740	0.0015765
B, equation (A.2)	3.82738	3.72667	3.73265
z, equation (9)	1.25865	1.23240	1.23395
ε_w, equation (10)	0.7252	0.7162	0.71677
$\vartheta_{w,o}$, equation (10)	26.843	27.031	27.019

Only two steps of iteration were necessary to attain the almost exact value (27.031 °C). Manufacturer claims $\vartheta_{w,o}$ = 27.0 °C.

For $\vartheta_{a,i}$ = 27 °C and ϑ_{WB} = 21.1 °C:

$$x_{a,i} = 0.01347 \text{ kg} \cdot \text{kg}^{-1},$$

so that, using equations (24) and (25), outlet air condition is obtained:

$$\vartheta_{a,o} = 34.35 \text{ °C and } x_{a,o} = 0.03460 \text{ kg} \cdot \text{kg}^{-1}.$$

(not available in manufacturer's bulletin!)

3) The wet bulb data are the same as in example 2. Also the calculating procedure is similar to the one used in that example, except that the cooling range is fixed at 10 °C (*table X*):

TABLE X
Iteratively calculated data in example 3.

Item	Step 1	Step 2	Step 3
Assumed value $\vartheta_{w,i}$	40.0	35.15	36.12
Assumed value $\vartheta_{w,o}$	30.0	25.15	26.12
b, equation (31)	0.0015535	0.0013523	0.0013889
B, equation (A.2)	3.67808	3.20175	3.28839
z, equation (9)	1.21973	1.09553	1.18812
ε_w, equation (10)	0.7118	0.6656	0.6744
$\vartheta_{w,i}$, equation (10)	35.15	36.12	35.93
$\vartheta_{w,o} = \vartheta_{w,i} - 10$ °C	25.15	26.12	25.93

(From the bulletin: $\vartheta_{w,i} \cong 35.8$ °C and $\vartheta_{w,o} \cong 25.8$ °C).

Outlet air: $\vartheta_{a,o}$ = 31.19 °C and $x_{a,o}$ = 0.02789 $kg \cdot kg^{-1}$.